Growth and Form of Planetary Seedlings: Results from a Sounding Rocket Microgravity Aggregation Experiment

Maya Krause

Astrophysikalisches Institut und Universitätssternwarte, Friedrich-Schiller-Universität Jena, Schillergässchen 2, 07745 Jena, Germany

Jürgen Blum*

Institut für Geophysik und Extraterrestrische Physik, Technische Universität zu Braunschweig, Mendelssohnstrasse 3, 38106 Braunschweig, Germany

(Received 6 February 2004; published 9 July 2004)

In a second microgravity experiment on the formation of dust agglomerates by Brownian motion-induced collisions we find that the agglomerates have fractal dimensions as low as 1.4. Because of much better data, we are now able to derive the diffusion constant of the agglomerates as a function of mass, to show that a power law with an exponent of 1.7 describes the temporal evolution of the mean agglomerate mass very well and to prove that the collision cross section is proportional to the geometrical cross section. In addition to that we derived the universal mass-distribution function of the agglomerates.

DOI: 10.1103/PhysRevLett.93.021103 PACS numbers: 96.35.Cp, 45.70.–n, 61.43.Hv, 81.10.Mx

It is still unknown how the micrometer-sized dust particles in the young solar system accumulated into 1-km-sized planetesimals, the first planetary bodies with substantial gravitational attraction, although in recent years considerable progress has been made in the understanding of the physics and dynamics of preplanetary dust agglomeration. The current knowledge is that dust grains stick to one another due to van der Waals forces [1] and form low-density fractal agglomerates when the collision velocities are sufficiently low [2–4]. For higher impact velocities, dust agglomerates are compacted or fragmented [2,4,5]. At the earliest stage of planet formation, the growth scenario is relatively simple when the μm-sized dust particles are so strongly coupled to the surrounding gas of the protoplanetary disk that the sole source for their mutual collisions and, hence, for agglomeration, is their thermal (Brownian) motion [6]. In a first paper [7], we reported on a microgravity experiment in which we experimentally simulated the Brownian-motion-driven agglomeration of micrometer-sized dust particles. Rapid formation of extremely fluffy, chainlike dust agglomerates was observed, but the sampling rate was too small so that many physical properties of the self-interacting cloud of dust agglomerates could not be derived.

In this paper, we report on a second microgravity experiment with a much higher sampling rate, which was carried out on board the sounding rocket Maser 8 in May 1999. The microgravity duration of the Maser rocket is 6 min, long enough for the evolution of dust agglomerates of considerable size, as shown in Ref. [7]. Very similar to the previous microgravity experiment, a sample of monodisperse, spherical SiO_2 dust grains with particle radii of $s_0 = 0.5$ μm was dispersed into a dilute gas of pressure $p \approx 2$ mbar and temperature $T = 300$ K.

The number densities, masses, structures, and motion of the dust particles and agglomerates in the sample were determined using high-speed, long-distance microscopy. With two orthogonally mounted microscopes with a field of view of 0.25×0.25 mm^2 and an experimentally determined depth of field of ~ 90 μm we continuously observed a subvolume of the dust cloud. Because of a bright-field illumination, the dust agglomerates were visible as darker-than-background silhouettes (see Fig. 1 in Ref. [7]). A more detailed description of the experimental setup and measurement technique can be found in Refs. [8,9].

For the determination of the mass of an individual dust agglomerate, we used the fact that the SiO_2 monomers were highly transparent. Hence, each individual microscopic glass bead inside a dust agglomerate absorbs the same amount of light, and the mass of an agglomerate can be determined by its total light absorption, even when the resolution of the long-distance microscope is too low to resolve single monomers. It turned out that we could reach a mass sensitivity that was better than the mass of a monomer grain, $m_0 = 1.0 \times 10^{-15}$ kg.

During the experimental run, the microscopes were continuously scanning through the dust cloud. Each of the 12 scans lasted 30 s and resulted in a total observational volume of 0.6 mm^3 for each microscope. As in the previous experiment, the dust cloud was not homogeneous and was slowly moving across the vacuum chamber with a constant velocity of (180 ± 20) μm s^{-1} due to thermophoresis. As a result of the dominating effect of thermal motion, the dust agglomerates were randomly oriented in space. Our data do not reveal any agglomerate alignment with respect to the direction of the drift motion.

Because of the low number of dust agglomerates, only an average diffusion constant for the ensemble of dust agglomerates could be derived in Ref. [7]. In the experiment

described here, the total number of dust agglomerates was sufficiently high to derive a mass dependency of the diffusion constant of fractal dust agglomerates. The diffusion constant D is related to the one-dimensional mean square displacement $\langle \Delta x^2 \rangle$ and the temporal difference in successive observations Δt by

$$\langle \Delta x^2 \rangle = 2D\Delta t\left[1 - \frac{\tau_f}{\Delta t} + \frac{\tau_f}{\Delta t}\exp(-\Delta t/\tau_f)\right] \quad (1)$$

[10]. Here, τ_f is the gas-grain response time. For the Epstein gas-drag regime (free molecular flow) that was present in the here-described experiments, the gas-grain response time is proportional to the mass m of the agglomerate (inertia) and inversely proportional to the agglomerate's geometrical cross section A (aerodynamic friction). The gas-grain response time in the free molecular flow regime is given by

$$\tau_f = \frac{1}{(4/3)(\delta P)\rho_g \bar{v}}\frac{m}{A}, \quad (2)$$

[11,12] with ρ_g, $\bar{v} = \sqrt{8kT/(\pi m_g)}$, δP, and k being the mass density of the gas, the mean thermal velocity of the gas molecules of mass m_g, a moment transfer coefficient which was experimentally determined for dust agglomerates to $\delta P = 1.11$ [12], and Boltzmann's constant, respectively. For the monomer grains and the gas properties in this experiment, we get $\tau_{f,0} = 0.898$ ms. Mind that, due to agglomeration, the response time of an aggregate, τ_f, will be changed with respect to the response time of the monomer grain, $\tau_{f,0}$. The time steps between observations in our experiment range from $\Delta t = 5$ ms to $\Delta t = 30$ ms. Thus, $\Delta t \gg \tau_{f,0}$ for most observation times and the term in the angular brackets in Eq. (1) is so close to unity that we get the classical expression for the diffusion equation

$$\langle \Delta x^2 \rangle = 2D\Delta t \quad (3)$$

[13]. As the diffusion constant and the gas-grain response time are related by

$$D = kT\frac{\tau_f}{m}, \quad (4)$$

a measurement of D yields an independent determination of the gas-grain response time τ_f. Figure 1 shows the measurements of the diffusion constants for dust agglomerates consisting between 2 and ~40 monomer grains. The different symbols in Fig. 1 represent the sampling times $\Delta t = 5, 10, \ldots, 30$ ms used for the determination of D in Eq. (3). There were sufficiently many dust agglomerates with small masses between 2 and 6 monomers in our sample so that the data points for these masses are averages of a single-mass sample. For the agglomerates with monomer numbers ≥ 7, the data points are logarithmic averages taken from dust agglomerates with similar masses.

The data in Fig. 1 show a steady decrease of the diffusion constant with increasing agglomerate mass.

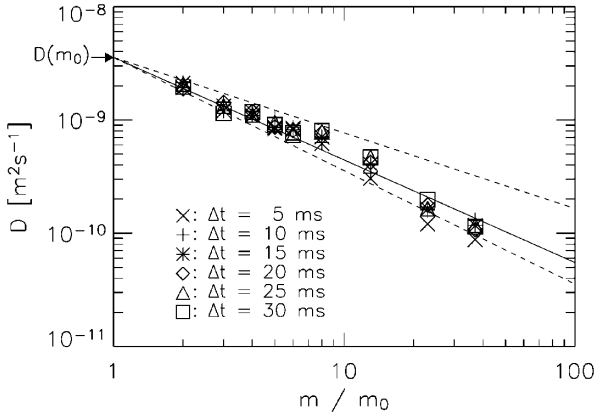

FIG. 1. Diffusion constant for fractal dust agglomerates of different masses. The different symbols mark measurement-time intervals of $\Delta t = 5, 10, \ldots, 30$ ms. The solid line is the best linear fit to the data and has a slope of $\alpha = -0.9$. The two dashed lines with slopes $-3/4$ and -1 mark the allowed range of diffusion constants for agglomerates. The arrow denotes the diffusion constant of monomer grains.

There is no systematic dependence of the diffusion constant on the sampling time, and a least-squares fit of all data points to a power law $D(m) = D(m_0)m^\alpha$ yields $\alpha = -0.91 \pm 0.14$ (solid line in Fig. 1) with a fixed best-guess value $D(m_0) = 3.56 \times 10^{-9}$ m^2 s^{-1} (arrow in Fig. 1). With Eqs. (2) and (4) we get

$$A(m) \propto m^{0.9}, \quad (5)$$

valid for fractal agglomerates with $D_f \approx 1.4$. Here, D_f is the fractal dimension of agglomerates following a mass-size relation $m/m_0 \propto r_g^{D_f}$, with r_g being the radius of gyration.

The above-mentioned fractal dimension of the agglomerates formed by pure Brownian motion was derived by plotting the agglomerate masses as a function of their two-dimensional radii of gyration r_g (Fig. 2) which were approximated by measuring the intensity distribution of the agglomerate images. Whenever multiple images of an agglomerate were available, we used the maximum value of the radius of gyration to compensate for projection effects. Because of the limited resolution of the long-distance microscope, the measured linear extent of small agglomerates was unrealistically high (crosses in Fig. 2) so that we restricted ourselves to agglomerate masses $m \geq 12\,m_0$ (square symbols in Fig. 2) for the determination of the fractal dimension.

It can be seen in Fig. 2 that for the larger dust agglomerates, the mass follows a power law of the maximum radius of gyration which gives a fractal dimension of $D_f = 1.41 \pm 0.06$ (solid line in Fig. 2). This value for the fractal dimension of the dust agglomerates is close to the earlier value of $D_f = 1.3$, indirectly determined in Ref. [7] by comparison of the internal mass distribution of a few agglomerates to agglomerates formed by computer simulations.

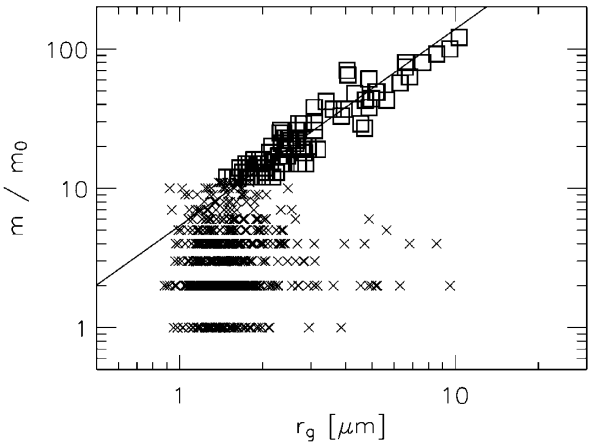

FIG. 2. Masses of fractal dust agglomerates as a function of the radius of gyration. Each symbol marks one dust agglomerate. For agglomerate masses $m/m_0 \geq 12$ (square symbols), the mass-size relation follows a power law with slope 1.41 (solid line) which we consider as the fractal dimension of the dust agglomerates. The finite resolution of the long-distance microscope disturbs the measurement of D_f for smaller agglomerates (crosses).

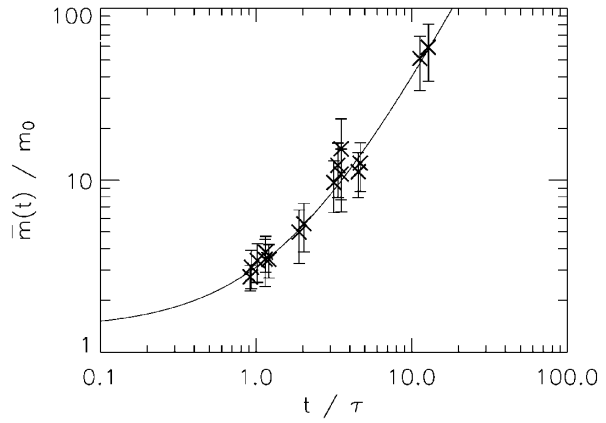

FIG. 3. Temporal evolution of agglomerate masses. Each data point represents the mean agglomerate mass observed at an average time t (in units of the monomer-collision time τ). The solid curve represents the best-fitting solution to a monodisperse growth [Eq. (6)].

The monomer number densities were constant in eight time intervals and ranged from $n_0 = 0.6 \times 10^{12}$ m^{-3} to 3.9×10^{12} m^{-3}. Each of these eight dust clouds was observed by two long-distance microscopes so that we get 16 dust-agglomerate samples. For each of those samples, we determined n_0, from which we derived the collision time scale for the monomer grains by

$$\tau = \frac{1}{n_0 \sigma_0 v_0},$$

with $\sigma_0 = 4\pi s_0^2$ and $v_0 = 4\sqrt{kT/\pi m_0}$ being the collision cross section and the mean thermal collision velocity of monomer grains, respectively. For each dust cloud, we determined the agglomerate-mass spectrum and the mean mass as a function of the average time t. The mass and time averages were derived by $\bar{m}(t) = [(\sum_{i=1}^{N} m_i^2)/(\sum_{i=1}^{N} m_i)]$ [14] and $t = [(\sum_{i=1}^{N} t_i)/N]$, respectively. Here, the index $i = 1, \ldots, N$ describes the ith dust agglomerate in the sample of a total of N agglomerates in each dust cloud. Thus, m_i and t_i are the mass and time of appearance of the ith dust agglomerate, respectively. Figure 3 shows the evolution of the mean agglomerate mass as a function of time in units of the monomer collision time τ.

In contrast to our earlier experiment [7], the new data span a much larger time interval $t/\tau = 0.9, \ldots, 13$. Figure 3 shows a steep increase of the mean agglomerate mass with time. To derive a quantitative dependence of $\bar{m}$ on t/τ, we fitted the mean-mass data to the theoretical function

$$\frac{\bar{m}(t)}{m_0} = \left[(1-\gamma)\left(a\frac{t}{\tau} + c\right)\right]^{1/1-\gamma}, \qquad (6)$$

derived in Ref. [2] for the pure monodisperse growth case. Here, a is the ratio between the theoretical and the experimentally determined monomer collision times, and c is a constant which determines the initial condition $\bar{m}(0)/m_0 = [(1-\gamma)\,c]^{1/(1-\gamma)}$. With a least squares fit to the data in Fig. 3 we get $a = 1.28 \pm 0.67$, $c = 2.05 \pm 1.15$, and $1/(1-\gamma) = 1.71 \pm 0.65$. The variable γ is theoretically determined by the relations

$$v(m) \propto \sqrt{\frac{kT}{m}} \propto m^{\beta}, \qquad \sigma(m) \propto m^{\delta}, \quad \text{and} \quad \gamma = \beta + \delta \qquad (7)$$

for ballistic collisions between the dust agglomerates or

$$D(m) \propto m^{\beta}, \qquad s(m) \propto m^{\delta}, \quad \text{and} \quad \gamma = \beta + \delta \qquad (8)$$

for diffusion-limited aggregation, with $v(m)$, $\sigma(m)$, $D(m)$, and $s(m)$ being the mean thermal collision velocity, collision cross section, diffusion constant, and size of agglomerates of mass m, respectively.

For $t = 0$, we get $\bar{m}(0)/m_0 = 1.36$ which is consistent with previous values of the mean initial mass [7]. For $t/\tau \gg 1$, the mean agglomerate mass follows a power law $\bar{m}(t)/m_0 \propto (t/\tau)^{1.7}$. Following Eqs. (7) and (8) and the results from this work, i.e., $D(m) \propto m^{-0.9}$ and $s(m) \propto m^{1/1.4}$, the theoretical exponent γ is given by $\gamma = \delta - 0.5$ for the ballistic case and $\gamma = -0.2$ for the diffusion-limited case. Unfortunately, the mass exponent of the collision cross section for agglomerates with very low fractal dimensions is unknown. A lower limit to the collision cross section is given by the geometrical cross section $A(m)$ [see Eq. (5)] so that $\delta \geq 0.9$. On the other hand, suprathermally rotating fractal dust agglomerates might have collision cross sections as high as $\sigma \propto s(m)^2$ so that we can assume $\delta \leq 1.4$. Hence, $0.4 \leq \gamma \leq 0.9$. For $t/\tau \gg 1$, the power law exponent in Eq. (6) should therefore have values of 0.83 for diffusion-limited growth and $1.7, \ldots, 10$ for ballistic growth. Because of the measured exponent of 1.71 in Eq. (6) we can exclude

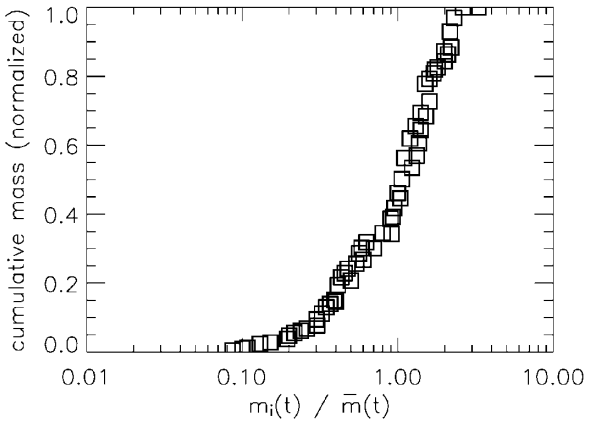

FIG. 4. Universal mass spectrum of the dust agglomerates grown by Brownian-motion-induced collisions. The normalized cumulative mass of the ensemble of dust agglomerates is shown as a function of the individual agglomerate masses $m_i(t)$ normalized by the mean agglomerate mass $\bar{m}(t)$ for all dust agglomerates with $t/\tau \geq 3$.

diffusion-limited growth for our experimental scenario and we can conclude that $\delta \approx 0.9$ so that $A(m) \propto \sigma(m)$ seems very well justified. Hence, we can exclude a considerable increase in collision cross section by suprathermal rotation. This is also supported by the continuous observation of the motion of individual dust agglomerates which showed only very slow rotation.

The most crucial assumption behind the derivation of Eq. (6) was the monodispersity of the agglomerates present in the ensemble. In this paper, we restrict ourselves to $t/\tau \gg 1$, for which the mass-distribution function should be self-preserving [14,15]. By numerical simulations of the Brownian agglomeration of dust, it was shown [14] that in this limit, a universal mass-distribution function exists, when the individual agglomerate masses m_i are substituted by $m_i(t)/\bar{m}(t)$, with the mean-mass function $\bar{m}(t)$ given by Eq. (6). In Fig. 4, we plotted the normalized cumulative mass distribution with $t/\tau \geq 3$.

The data points fall onto a well-defined S-shaped curve. It should be mentioned that due to the limited observational volume, the shape of the cumulative-mass curve towards the upper mass end might be influenced by small-number statistics of large dust agglomerates. The central 50% (90%) of the mass-distribution function in Fig. 4 comprise dust agglomerates in the mass range $0.5 \lesssim m_i/\bar{m} \lesssim 1.5$ ($0.2 \lesssim m_i/\bar{m} \lesssim 2.3$) so that we can conclude that the condition of quasimonodispersity is sufficiently well satisfied. A comparison of the widths of the experimental with the theoretical self-preserving mass spectrum in Ref. [14] shows good agreement. However, the width of the experimental mass distribution function is much narrower than the ones theoretically derived in Ref. [15] for $D_f = 2, \ldots, 3$.

In this paper, we presented the results of a second microgravity experiment on the agglomeration of micron-sized dust particles due to Brownian motion. With the new data, we could show that the diffusion constant of low-fractal-dimension dust agglomerates scales almost inversely proportional to the agglomerate mass. The fractal dimension of the agglomerates that form due to sticking collisions were found to be $D_f \approx 1.4$ which is close to the value suggested in Ref. [7]. The temporal evolution of the mean mass of the agglomerate sample could be followed over an extended time range. It turned out that an analytic approximation to the growth equation fits the data very well. The ultimate power law of the growth curve with an exponent of ~ 1.7 can be explained by ballistic, rather than diffusion-limited, agglomeration and a collision cross section of the dust agglomerates that is proportional to the geometrical cross section. The justification of the approximate validity of the analytical solution is given by the quasimonodispersity of the sample of dust agglomerates as shown by the universal mass-distribution function in Fig. 4.

This work was supported by the European Space Agency (ESA) and by the German Space Agency (DLR) under Contract No. 50 WM 0036.

*To whom correspondence should be addressed.
Email address: j.blum@tu-bs.de

[1] L. Heim, J. Blum, M. Preuss, and H.-J. Butt, Phys. Rev. Lett. **83**, 3328 (1999).
[2] J. Blum, in *Astrophysics of Dust*, edited by A. Witt, G. Clayton, and B. Draine, ASP Conference Series Vol. 309 (The Astronomical Society of the Pacific, San Francisco, 2004), p. 369.
[3] G. Wurm and J. Blum, Icarus **132**, 125 (1998).
[4] J. Blum and G. Wurm, Icarus **143**, 138 (2000).
[5] C. Dominik and A. G. G. M. Tielens, Astrophys. J. **480**, 647 (1997).
[6] S. J. Weidenschilling and J. N. Cuzzi, in *Protostars and Planets III*, edited by E. Levy and J. I. Lunine (University of Arizona Press, Tucson, 1993), p. 1031.
[7] J. Blum *et al.*, Phys. Rev. Lett. **85**, 2426 (2000).
[8] J. Blum, G. Wurm, and T. Poppe, Adv. Space Res. **23**, 1267 (1999).
[9] R. H. Huijser, E. G. van der Sar, R. Schelling, and C. Rens, in *Proceedings of the ESA Symposium on European Rocket and Balloon Programmes and Related Research, Potsdam, Germany, 1999*, edited by B. Kaldeich-Schürmann (ESA Publications, Noordwijk, 1999), p. 511.
[10] S.W. Gardiner, *Handbook of Stochastic Methods for Physics, Chemistry, and the Natural Sciences* (Springer, Berlin, 1985).
[11] P. S. Epstein, Phys. Rev. **23**, 710 (1924).
[12] J. Blum, G. Wurm, S. Kempf, and T. Henning, Icarus **124**, 441 (1996).
[13] A. Einstein, Ann. Phys. (Leipzig) **17**, 549 (1905).
[14] S. Kempf, S. Pfalzner, and T. Henning, Icarus **141**, 388 (1999).
[15] S. Vemury and S. E. Pratsinis, J. Aerosol Sci. **26**, 175 (1995).